



ISSN: 2617-6548

URL: www.ijirss.com

Real-time frequency stabilization of standalone PV system with SMC

 Nisha Gnanam^{1*}, Jamuna Kamaraj²

^{1,2}*School of Electrical Engineering VIT Chennai, India.*

*Corresponding author: Nisha Gnanam (Email: nishagnanam@gmail.com)

Abstract

This paper aims to obtain suitable control for the Standalone Photo Voltaic (SAPV) system to meet consumer demands in weather conditions. A SAPV system is developed with a solar array with Maximum Power Point Tracking (MPPT), a Boost converter, and an inverter. This system uses controllers for maximum power output tracking, constant DC output of the Boost converter, and constant output voltage and frequency with Pulse Width Modulation (PWM) control mode. MPPT, boost converter, and inverter controller parameters are designed and tuned, respectively. Proportional gain (K_p) and Integral gain (K_i) values and the Sliding Mode Method (SMC) tune the controller parameters. The innovative aspect of this work is to propose a standalone PV system with controllers based only on the sliding mode control approach. Moreover, the current controller provides an output current of high quality with a THD of 1.6 %. Effectiveness and robustness of the proposed scheme modeled and simulated under OPAL-RT real-time Software in Loop (SIL) platform with MATLAB Simulink under fast variations of irradiance and temperature. Various analyses have been carried out for examining the proposed Sliding Mode Controller-based standalone photovoltaic system.

Keywords: Boost converter, Controllers, Maximum power point tracking, Opal RT, Photo voltaic, Sliding mode controller, Standalone.

DOI: 10.53894/ijirss.v6i1.1080

Funding: This study received no specific financial support.

History: Received: 13 July 2022/**Revised:** 26 November 2022/**Accepted:** 9 December 2022/**Published:** 19 December 2022

Copyright: © 2023 by the authors. This article is an open access article distributed under the terms and conditions of the Creative Commons Attribution (CC BY) license (<https://creativecommons.org/licenses/by/4.0/>).

Authors' Contributions: Both authors contributed equally to the conception and design of the study.

Competing Interests: The authors declare that they have no competing interests.

Transparency: The authors confirm that the manuscript is an honest, accurate, and transparent account of the study; that no vital features of the study have been omitted; and that any discrepancies from the study as planned have been explained.

Ethical Statement: This study followed all ethical practices during writing.

Publisher: Innovative Research Publishing

1. Introduction

Owing to increasing fuel costs and ecological anxiety, Renewable Energy Sources (RES) are the primary sources for all power sectors. Renewable energy sources include wind, hydro, geothermal, and solar. Limitless characteristics and a clean environment are the output of power generation with renewable energy sources. These energies double-deal with innovative technology and provide remarkable profit improvements [1]. Light energy is economical and fast-developing technology [2]. Photovoltaic (PV) systems are cost-effective and have competing capabilities among conventional power systems.

On the other hand, the disadvantages of this system are non-linear performance for PV characteristics and low efficiency (9 to 16 in percentage). In order to remedy the aforementioned disadvantages, different answers are discussed for PV system performance improvement. One of the best solutions for this condition is implementing the MPPT technique,

which provides an ideal answer for the PV module's optimal point. In Mehdipour and Mohammadi [3], Chaibi, et al. [4] discussed numerous PV applications that used different types of MPPT algorithms [3, 4].

Perturb and Observe (P&O) is a common method in the MPPT technique. The algorithm method depends on input current or voltage perturbing and observing system response until the PV module is optimal. Moreover, the P&O has an easy algorithm that assists implementation. However, its performances are particularly analyzed, the Maximum PowerPoint around oscillation [5, 6]. The activity of low irradiance changes. It is very difficult to decide on the MPP at the correct location, which makes it happen to decrease the PV's overall efficiency and power loss. MPPT techniques have been proposed to overcome these difficulties, depending on artificial intelligence [7, 8] and genetic algorithms [9]. These methods provide good evidence for high superiority for tracking MPP when reaching the Maximum power instantaneously despite environment change conditions and steady-state without oscillation.

To provide the benefits for non-linear controllers, good efficiency, simplicity, and fast response, back-stepping and sliding mode (SM) is used [10]. The simple implementation provides robust performance in opposition to the external disturbances for PV different applications by using these controllers. The Sliding Mode [SM] method applies the non-linear control strategy resulting from the Variable Structure System (VSS). Accordingly, the PV system used switched-mode converters for this controller [10, 11]. Moreover, an inverter or DC-DC converter, SMC, has been utilized. Levron and Shmilovitz presented [12] SM to MPPT and controlled the IGBT switches; the aim is to control the inverter to connect through the grid followed by the reference current. The paper [13] proposed a Grid-connected single-phase system with a proposed sliding mode to decrease the overshoot current and contribute to the components' optimal designs.

The author Tsai and Chen [14] discussed a DC-DC Boost converter with R-load by using sliding mode control in a finite time; the result provides a fast response time and high stability. Nonetheless, the double-dealing system of PV is connected with DC loads. In such circumstances, author Laura et al. utilized the adaptive controller of the Sidling Mode method to deal with two different converters to control a Grid-connected PV system. Due to irradiance changes, these converters are controlled with robust properties and respond quickly.

Because of these advantages of the Sliding Mode Controller (SMC), namely fast response and robustness, most papers utilised these controllers for grid-connected PV systems [13, 15]. Most authors discussed sliding mode controllers in a grid-connected power system due to fast response, maintaining stability, and consistent performance. The important advantage of the sliding mode controller is its insensitivity to variations of parameters and disturbances. Therefore, our system was designed and evaluated in a standalone PV system Figure 1 with the help of two-stage converters. These two stages of converters follow the following principles;

- (i) The first step is custom-made surface must be designed. The Photo Voltaic array with the sliding mode method in MPPT provides the command signal to the DC-DC boost converter. So duty cycle quickly obtains the MPP.
- (ii) The second step is the feedback controller or control law implementation. Here, the current controller depends upon the inverter's Pulse Width Modulation (PWM), which moves in the load and determines the current reference.

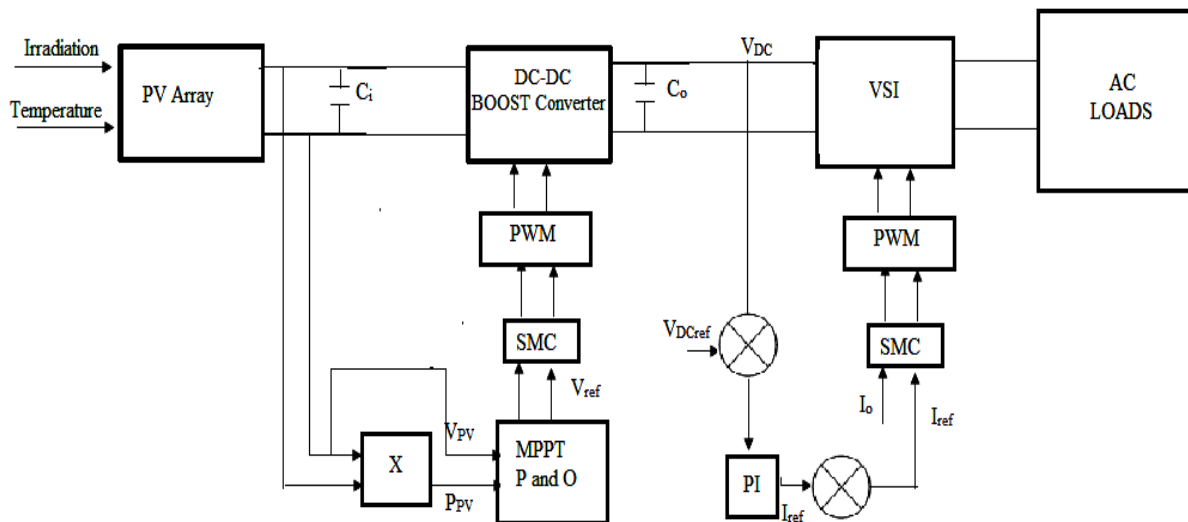


Figure 1. Overall structure of SAPV system using PWM-based SMC.

Irradiation is considered a perturbation in the design of the proposed controllers as it affects the overall efficiency of the SAPV. It is simulated under quick transformation in solar irradiance and temperature to validate the functioning and stability of the suggested system.

The paper is divided into the following sections: Section 2 discusses the proposed SAPV system's mathematical design of the PV cell. Sections 3 and 4 discuss MPPT and current controller works with SMC. The simulation outputs and analysis are presented in section 5. Section 6 is the last section, and it is devoted to the conclusion and summary.

2. Modeling of the Components

(a). PV Array Model

The majority of solar panel comprises a series of cells. A p-n junction, which produces electricity, can depict this cell. Different equivalent circuits were exploited to inspect the electrical performance of PV cells when light is reflected off of them. In literature, [16, 17] models are mentioned.

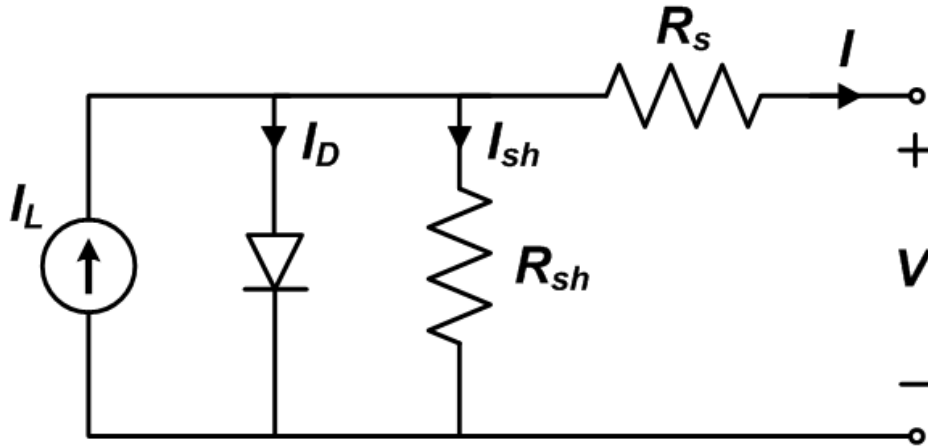


Figure 2.
Single diode PV cell.

Figure 2 represents the commonly used model for PV cell configurations; it provides good performance during high-temperature changes and irradiance.

The output current is based on three different currents, namely photocurrent (I_{PH}), Diode Current (I_D), and shunt current (I_{SH}) which are proportional to the irradiance, temperature, and resistance respectively. The output current is normally based on I_{PH} , whereas the photocurrent increases with irradiance,

$$I_{PV} = I_{PH} - I_D - I_{SH} \tag{1}$$

Calculation of the Diode forward current:

By applying the Shockley diode equation, we get,

$$I_D = I_S(e^{\frac{V_D}{nV_T}} - 1) \tag{2}$$

From Equation 2 we get,

$$I_D = I_0(e^{\frac{V_o}{nV_T}} - 1) \tag{3}$$

The ideality factor indicates “n”. The values vary from 1 to 2 based on the fabrication process; in many conditions, the value is assumed to be 1.

The thermal voltage $V_T = (KT/q)$

Where K is Boltzmann Constant, the value is (1.38×10^{-23}) J/K, PN junction absolute temperature is denoted by T, and q is a charge of an electron (1.602×10^{-19}) .

The light-generated current I_{PH} variations based on the calculated temperature and irradiance are calculated as follows;

$$I_{PH} = I_{SC} + K_i(T - T_{ref}) \frac{\lambda}{\lambda_{ref}} \tag{4}$$

The following Table 1 provides the specifications of the PV system.

Table 1.
PV system specifications.

Parameters	Values
Open circuit voltage (V_{oc})	64.2 V
Short circuit current (I_{sc})	5.96 A
Voltage in maximum PowerPoint (V_{MPP})	54.7 V
Current in maximum PowerPoint (I_{MPP})	5.58 A
Number of cells connected per module	96
Power tolerances	$\pm 5\%$

The panels are arranged parallel and in series for various PV applications based on the used voltage and required power. PV cell mathematical modelling aims to obtain the accurate output characteristics of current (I) and voltage (V) and plot the I-V and P-V Figure 2.

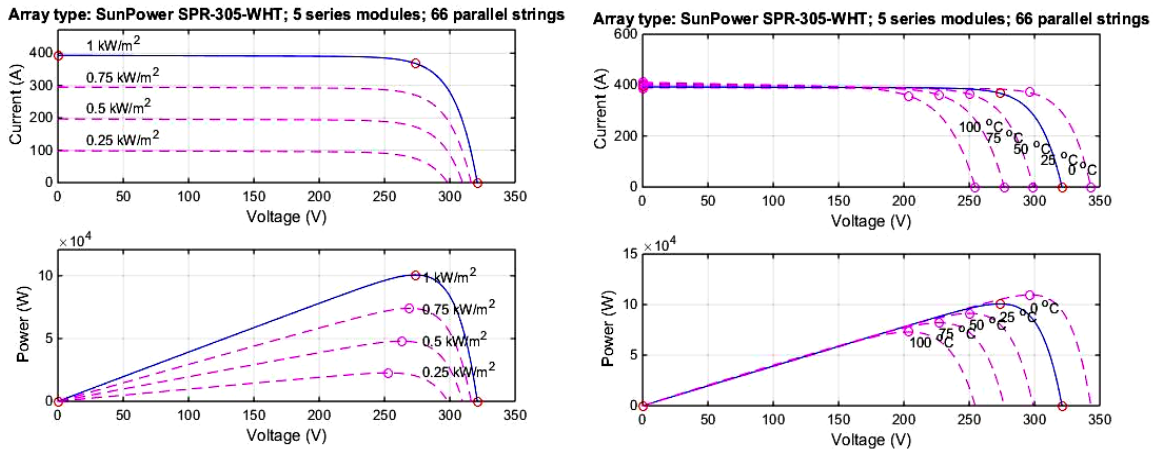


Figure 3. SAPV characteristics for I-V and P-V (a) changing irradiation and (b) changing temperature.

Figure 3(a) shows the changing irradiation (250W/m², 500W/m², 750W/m², and 1000W/m²) with respect to constant temperature 25°C. The Standard Test Condition power rating value for this system is 305 Watts; Standard Test Condition (STC) power per area is 187.0W/m². Figure 3(b) above shows the changing temperatures are 0°C to 100°C to constant irradiation 1000 W/m².

3. Design of the Controller

(a). MPPT with SMC

In this, maximum power point operation is very important in PV systems. The derivative of power concerning voltage, i.e., $[\frac{\partial P_{pv}}{\partial V_{pv}}]$ must converge to zero for the PV panel's P-V characteristic to be performed at its MPP [18]. As illustrated in Figure 4, the sliding mode concept technique generates the rule that operates the DC-DC boost converter duty cycle α_1 .

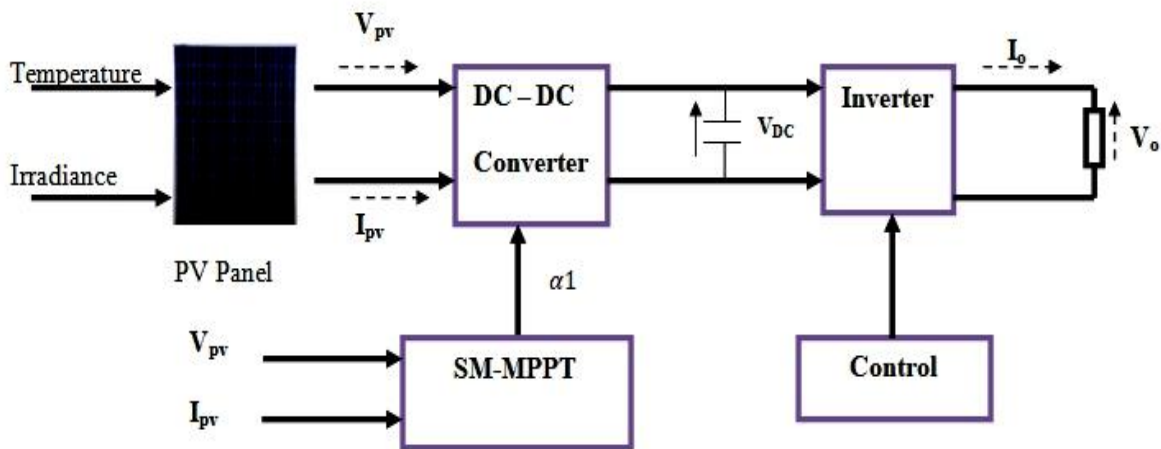


Figure 4. Maximum PowerPoint Tracking using SMC.

There are two steps presented in SMC. The initial step of sliding mode is to design the control rule for sliding surface selection; the variable references and state variables are collected by surface. When PV power gets maximized, the sliding surface is selected as follows,

$$\sigma_1 = e_1 + \gamma_1 e_1 \tag{5}$$

Where,

$$e_1 = \text{dynamic error relating to the reference value and regulated output}$$

We get,

$$e_1 = \gamma_1 = \partial P_{pv} / \partial V_{pv} \tag{6}$$

γ_1 = positive polynomial parameter.

Hence, the surface time derivative is written as,

$$\dot{\sigma}_1 = \dot{e}_1 + \dot{\gamma}_1 e_1 \tag{7}$$

The main benefit of this technique is its robust and stable behaviour. The Lyapunov function proves that this intensity is proportional to the good looks of the surface. So, with the help of the Lyapunov function represented by the following equation,

$$V_1 = \frac{1}{2} \sigma_1 \tag{8}$$

The above Equation 8 is less than zero due to asymptotic stability present in the balancing point; therefore, it can be written as follows,

$$V_1 = \sigma_1 \dot{\sigma}_1 \tag{9}$$

Considering the dynamic function, it can be written as

$$\dot{\sigma}_1 = -\lambda_1 |\sigma_1| \tag{10}$$

From Equation 10, the Lyapunov condition λ_1 should be positive. Then, the control law is based on the deviation of the PV current & voltage (I_{PV} , and V_{PV}) and based on irradiance and temperature varying. In this, the robust feature of the SM-MPPT provides consistent performance even with parametric variations. In references, many authors proved MPPT depends on SM utilized for I_{PV} reduced equation to shorten the calculations.

Calculations for PV current Equation:

$$\frac{\partial I_{PV}}{\partial V_{PV}} = \frac{-A I_{Os} \exp[A(V_{PV} + R_S I_{PV})] - \left(\frac{1}{R_{sh}}\right)}{1 + \left(\frac{R_S}{R_{sh}}\right) + R_S A I_{Os} \exp[A(V_{PV} + R_S I_{PV})]} \tag{11}$$

Assume $H = 1 + \left(\frac{R_S}{R_{sh}}\right) + R_S A I_{Os} \exp[A(V_{PV} + R_S I_{PV})]$

So we obtained,

$$\frac{\partial I_{PV}}{\partial V_{PV}} = \frac{-A I_{Os} \exp[A(V_{PV} + R_S I_{PV})] - \left(\frac{1}{R_{sh}}\right)}{H} \tag{12}$$

Applying the second derivative to the current equation, we get

$$\frac{\partial^2 I_{PV}}{\partial V^2_{PV}} = \frac{-A^2 I_{Os} \exp[A(V_{PV} + R_S I_{PV})] \left(R_S \left(\frac{\partial I_{PV}}{\partial V_{PV}}\right) + 1\right)}{H^2} \tag{13}$$

$$\frac{\partial^3 I_{PV}}{\partial V^3_{PV}} = \frac{A^3 I_{Os} \exp[A(V_{PV} + R_S I_{PV})] \left(R_S \left(\frac{\partial I_{PV}}{\partial V_{PV}}\right) + 1\right)^2}{H^3} - \frac{\left(\frac{\partial^2 I_{PV}}{\partial V^2_{PV}}\right) \{R_S A^2 I_{Os} \exp[A(V_{PV} + R_S I_{PV})]\}}{H^3} + \frac{2A^3 I_{Os}^2 R_S^2 \exp^2[A(V_{PV} + R_S I_{PV})] \left(R_S \left(\frac{\partial I_{PV}}{\partial V_{PV}}\right) + 1\right)}{H^3} \tag{14}$$

Power with respect to voltage, we get,

$$\frac{\partial P_{PV}}{\partial V_{PV}} = I_{PV} + V_{PV} \frac{\partial I_{PV}}{\partial V_{PV}} \tag{15}$$

$$\frac{\partial^2 P_{PV}}{\partial V^2_{PV}} = 2 \frac{\partial I_{PV}}{\partial V_{PV}} + V_{PV} \frac{\partial^2 I_{PV}}{\partial V^2_{PV}} \tag{16}$$

$$\frac{\partial^3 P_{PV}}{\partial V^3_{PV}} = 3 \frac{\partial^2 I_{PV}}{\partial V^2_{PV}} + V_{PV} \frac{\partial^3 I_{PV}}{\partial V^3_{PV}} \tag{17}$$

$$\dot{y}_1 = \frac{\partial y_1}{\partial t} = \frac{\partial^2 P_{PV}}{\partial V^2_{PV}} \frac{\partial V_{PV}}{\partial t} \tag{18}$$

$$\ddot{y}_1 = \left(\frac{\partial^3 P_{PV}}{\partial V^3_{PV}}\right) \left(\frac{\partial V_{PV}}{\partial t}\right)^2 + \left(\frac{\partial^2 P_{PV}}{\partial V^2_{PV}}\right) \left\{ \frac{1}{LC} \left(\frac{\partial I_{PV}}{\partial V_{PV}}\right) \left(\frac{\partial V_{PV}}{\partial t}\right) - \frac{1}{LC} (V_{PV} - V_{DC}) \right\} - \alpha_1 \left(\frac{V_{DC}}{LC}\right) \frac{\partial^2 P_{PV}}{\partial V^2_{PV}} \tag{19}$$

The above equation may be written as follows $E + \alpha_1 K$,

Where,

$$E = \left(\frac{\partial^3 P_{PV}}{\partial V^3_{PV}}\right) \left(\frac{\partial V_{PV}}{\partial t}\right)^2 + \left(\frac{\partial^2 P_{PV}}{\partial V^2_{PV}}\right) \left\{ \frac{1}{LC} \left(\frac{\partial I_{PV}}{\partial V_{PV}}\right) \left(\frac{\partial V_{PV}}{\partial t}\right) - \frac{1}{LC} (V_{PV} - V_{DC}) \right\}$$

$$K = \left(\frac{V_{DC}}{LC}\right) \frac{\partial^2 P_{PV}}{\partial V^2_{PV}}$$

By using \dot{y}_1 and \ddot{y}_1 equation in $\dot{\sigma}_1$ also using $\dot{\sigma}_1 = -\lambda_1 |\sigma_1|$, the control law should come following the equation,

$$\alpha_1 = \frac{-\lambda_1 |\sigma_1| - \dot{y}_1 e_1 - E}{K} \tag{20}$$

(b). Output Current Controller with SMC

Energy conversion of Direct Current (DC) to Alternating Current (AC) conversion is a difficult and important task in a power system. It is one of the primary solutions for running a standalone PV system on AC. Furthermore, the sliding mode technique is used to convey the maximum quantity of energy from the DC bus to the load. The sliding surface design is the first step in designing the output current controller. The divergence among the state variable and its reference values [19] defined the sliding surface in general.

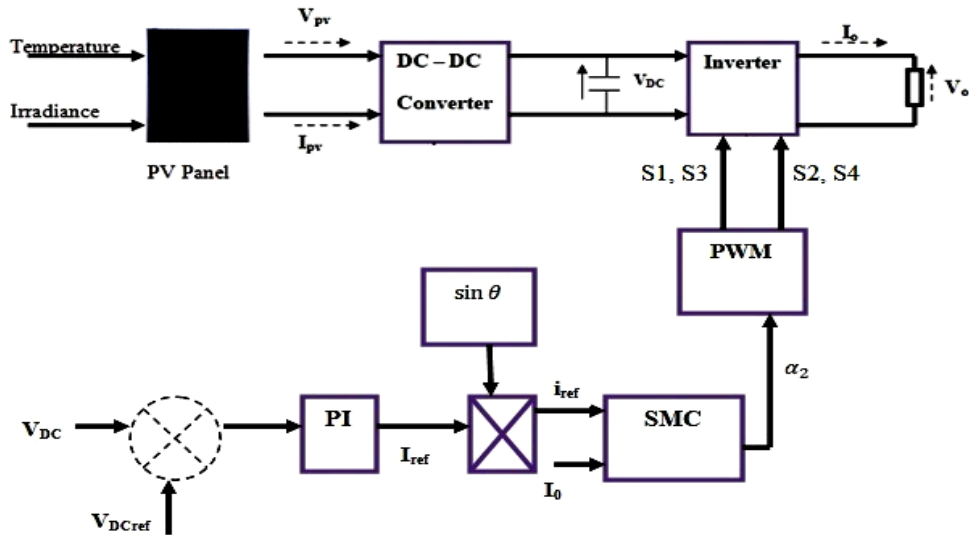


Figure 5. Control strategy for output controller using sliding mode controller.

The DC-DC boost converter is connected to the AC inverter. The three-phase inverters are used for high-power applications. An Insulated-Gate Bipolar Transistor (IGBT) switch used for inverter design, compared to other switches, provides fast switching and high voltage capability. The advantages of the sliding mode controller are fast response, simplicity, and high accuracy for tracking system response. The controller controlling technique for switching frequency is constant, based on modified bandwidth. The proposed control strategy for the output controller using a sliding mode controller is shown in Figure 5. The control strategy for the output controller using a sliding mode controller determines the I_{ref} peak current with the help of the PI loop, which it presents among the V_{DC} and V_{DCref} . In addition, I_{ref} is multiplied by the generated value of $\sin \omega t$ to determine sinusoidal reference current i_{ref} .

The sliding surface current equation is designed as per the following equation, based on low-frequency sensibility,

$$\sigma_2 = i_o - I_{ref} \sin(\omega t) \tag{21}$$

We made the switching surface stable by using the Lyapunov equation [$V_1 = \frac{1}{2} \sigma_1$] and substituted $\dot{\sigma}_1 = -\lambda_1 |\sigma_1|$ in the control law Lyapunov derivative function to obtain α_2

$$\alpha_2 = \frac{1}{2} \left\{ 1 + \frac{-L_0 \lambda_2 \text{sign}(\sigma_2) + (R_0 + R_C) + L_0 \left(\frac{\partial i_{ref}}{\partial t} \right)}{V_{DC}} \right\} \tag{22}$$

Where, $\frac{\partial i_{ref}}{\partial t} = I_{ref} \omega \cos \omega t$

According to the Lyapunov stability condition

$\dot{V}_2 = -\lambda_2 |\sigma_2|$, the λ_2 coefficient should be zero.

4. Real-Time Simulation of the Controller for SAPV

The simulation model of the 100kW SAPV system simulated OPAL-RT (Real Time) with MATLAB software. Simulating time steps are fixed at 50 μ s. The PV array delivers the maximum power at 1000w/m² solar radiation and 25°C temperature. The system was tested and simulated in real time.

Table 2. Controller parameters for the PV system.

Controllers	Parameters	Values
Sliding mode controller	λ_1	5000
	λ_2	500
	γ_1	150
PI controller coefficients	K_p	0.85
	K_i	0.001
	Frequency(Hz)	50
	ω (rad/sec)	314.16

Table 2 presents the controller parameters for the standalone PV system. The PI controller parameter values are K_p is 0.85 and K_i is 0.001.

5. Results and Discussion

This section deals with evaluating the proposed controllers in a PV system. The SAPV system has been developed in MATLAB Simulink with OPAL-RT hardware implementation.

5.1. P and O MPPT with PI Controller

Condition: 1 Changing irradiation and Temperature in SAPV using a PI controller with an MPPT algorithm

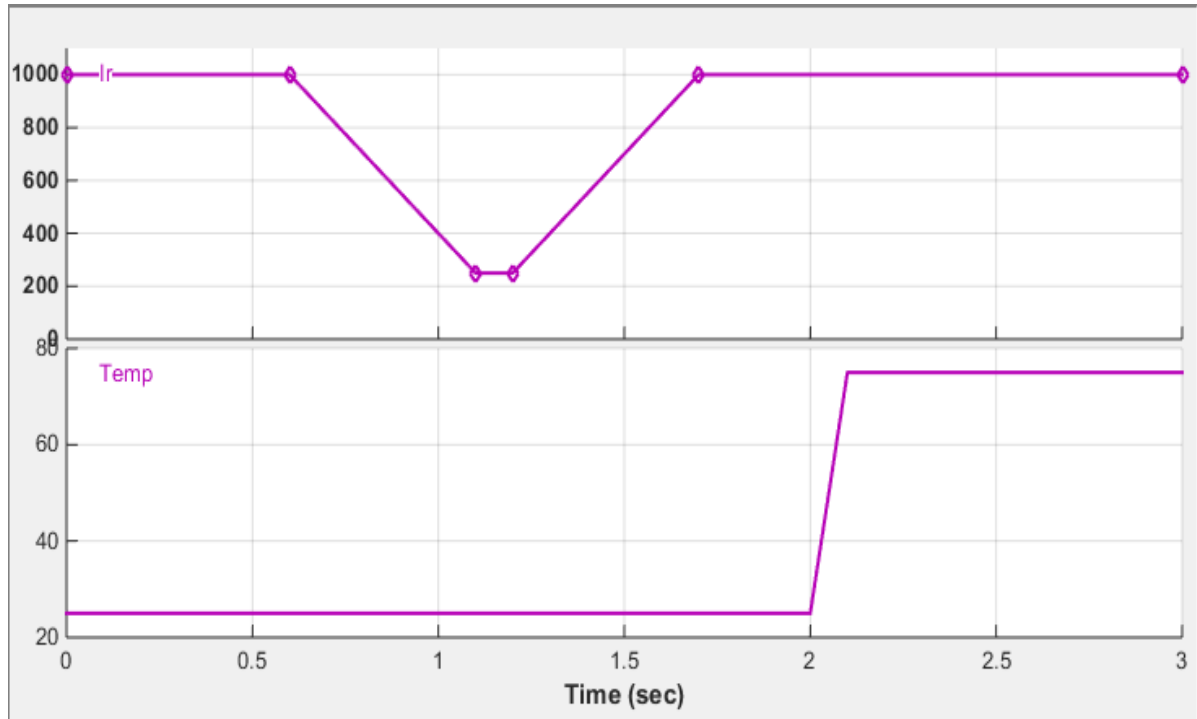


Figure 6. Irradiation and Temperature used in the simulation.

Figure 6 shows the irradiation and temperature used in SAPV in Real-time simulation.

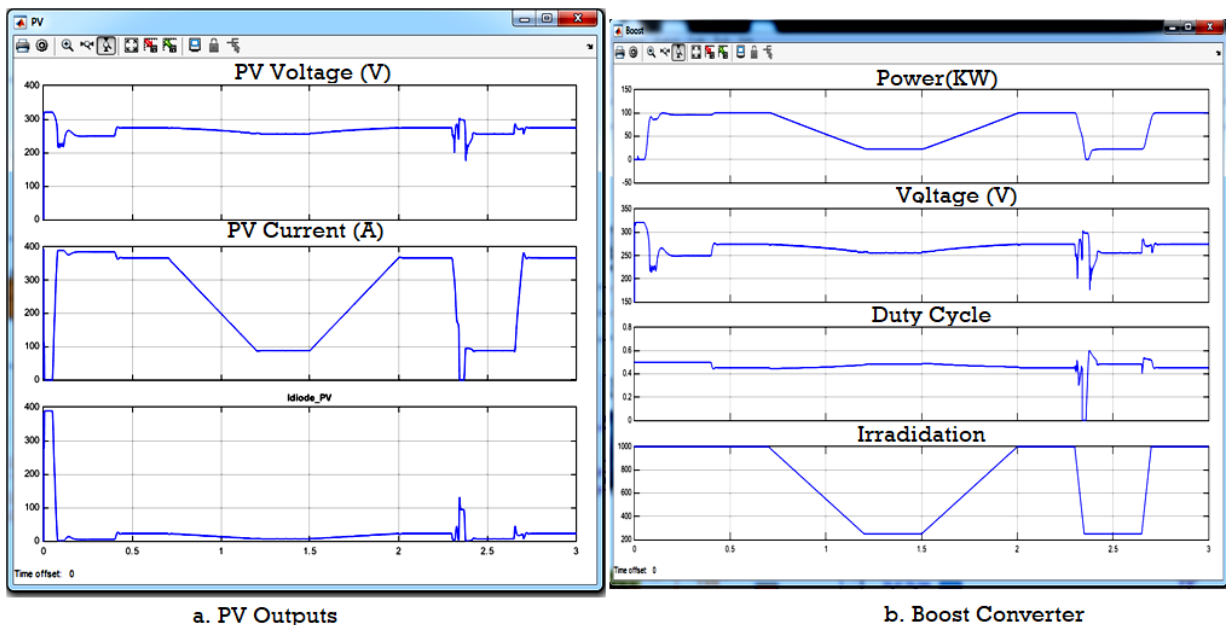


Figure 7. Simulation output for changing temperature and irradiation (a) shows the PV output (b) Boost converter simulation output.

Figure 7(a) above shows the PV voltage, current, and PV Diode current characteristics for Figure 6. Also, the output voltage of the PV system was boosted to 500V with the help of the following design parameters of the boost converter: $L = 5\text{mH}$, $C_{in} = 100\mu\text{F}$, and $C_{out} = 12\text{mF}$. The duty cycle was generated by the P and O MPPT algorithm regarding changing PV irradiance in Figure 7. The boost converter PV voltage, power, and duty cycle result are shown in Figure 7(b).

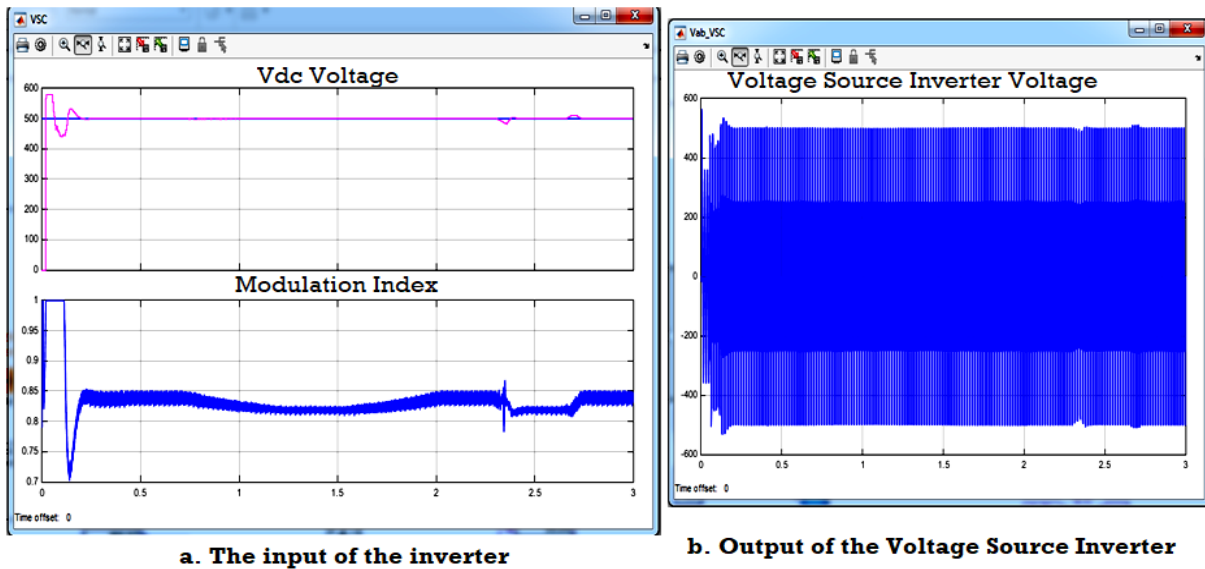


Figure 8.
Simulation results (a) The input of the inverter (b) Output of the VSC

The boost converter's output is connected through the Voltage Source Converter (VSC), which converts the unidirectional voltage supply to a bidirectional output supply. Here, the PWM reference voltage is set as 500 Volt. The VSC inverter is used to control the amplitude of the sinusoidal signal's output concerning the modulation's width. Hence, the VSC reference voltage and modulation index output are shown in Figure 8(a). Figure 8(b) represents the output of the sinusoidal waveform of V_{ab_VSC} .

5.2. Case Study: SAPV System Tuned by SMC

In the section, the parameters are tuned with the help of adaptive controllers for different atmospheric conditions to get the constant voltage and frequency. Also, the steady-state error is zero. Condition: 1 Constant Temperature and Constant irradiance

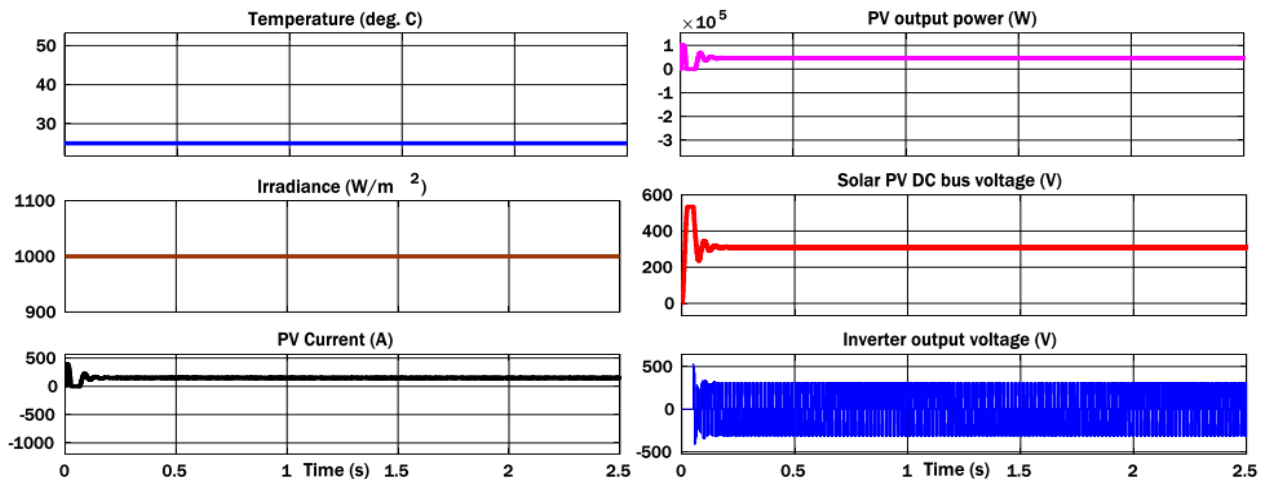


Figure 9.
PWM-based SMC under constant temperature and constant irradiance.

Figure 9 above shows that the output graph presents the output power, current, and voltage of the SAPV system at constant temperature and irradiance (25°C & 1000W/m²). The result reveals that the SMC controls the settling time, and oscillation is far less. However, the transient period was perceived at the time interval of 0 to 0.2 sec with marginal overshooting.

Condition: 2 Different irradiance and Constant Temperature

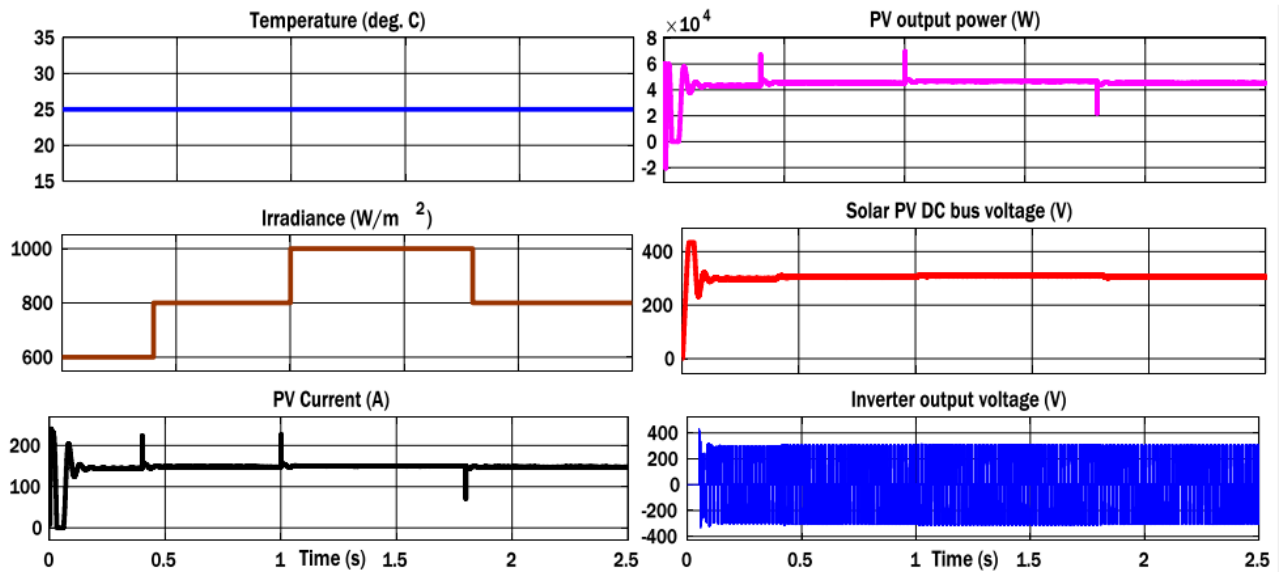


Figure 10. Simulation output for SAPV using SMC constant temperature and Different irradiance.

Figure 10 above shows SMC-based SAPV for constant temperature and different irradiance conditions. During 0 to 2.5 sec, the graphs show SAPV current and power response. The simulation achieves a smooth transient response in PV results: output power, current, DC bus voltage, and inverter output voltage. Under the different irradiance, the controller can maintain a constant DC bus voltage with SMC.

Condition: 3 Different temperatures and Constant irradiance.

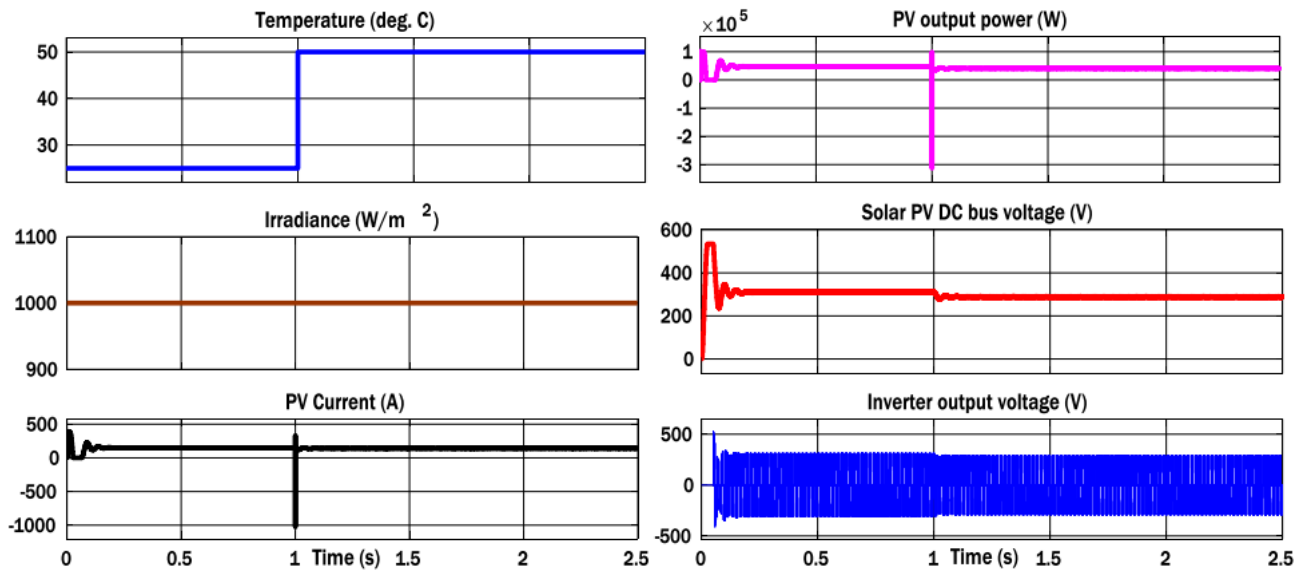


Figure 11. PWM-based SMC under different temperatures and constant irradiance.

PWM-based SMC under different temperatures and constant irradiance results are shown in Figure 11. The temperature ranges vary from 25°C to 50°C, and irradiance is fixed at 1000W/m². The simulation outputs clearly show smooth current and power output waveform transitions in different temperatures. Also, the DC bus voltage remains constant. While changing the temperature, the output voltage of the inverter is stable.

Condition: 4 Different temperatures and Different Irradiance

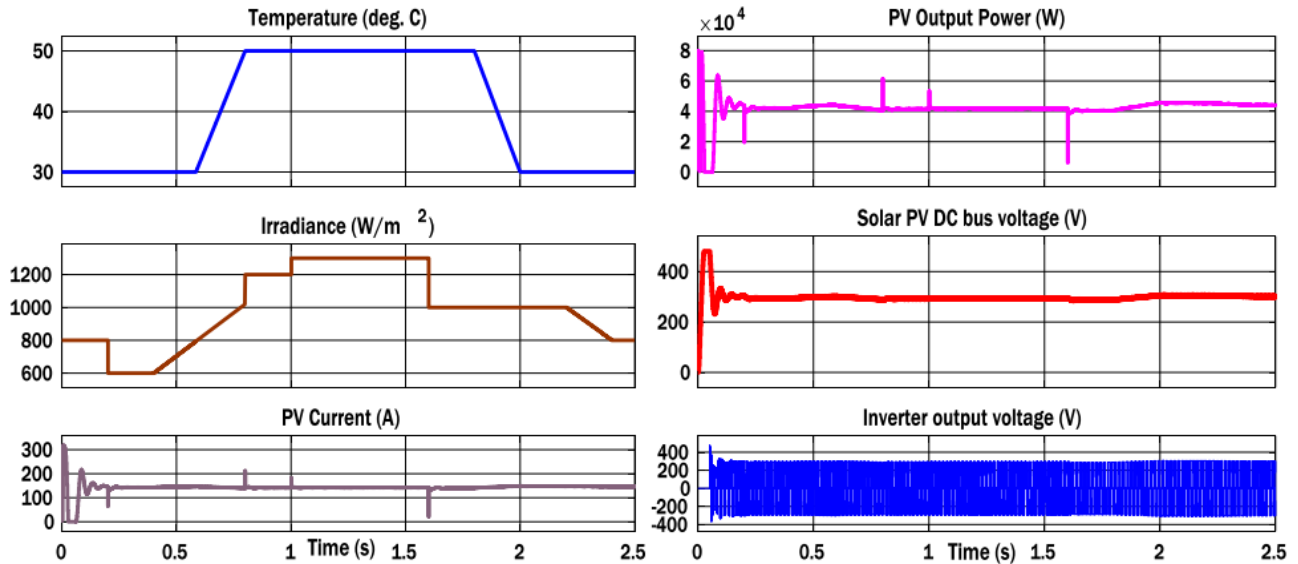


Figure 12. PWM-based SMC under different temperatures and different irradiance.

Figure 12 shows PWM-based SMC under different temperatures and different irradiance. In this condition, the temperature and irradiance vary simultaneously. When sudden changes happen in the irradiation, the system reacts appropriately. The simulation output shows less number of spears, constant DC voltage, and inverter voltage well synchronized.

6. Conclusion

The adaptive controller is based on the SMC applied for a SAPV system. The proposed controller consists of Sliding Mode in Maximum Power Point Tracking and outputs the current controller in the system. Moreover, the current reference generation is performed directly from the Proportional Integral (PI) controller. In any critical situation with sudden changes in the weather condition, the controllers respond fast to attain the reference value lacking fluctuation around the MPPT method. Our proposed technique provides stable reference values healthier than the traditional ones depending on the variable steps. The system is stable due to the Lyapunov function. The controller performance is verified through mathematical and real-time simulations; the PV system results show superior and high steadiness. Hence, from the real-time analysis, SMC-based MPPT provides high steadiness and fast reaction through changes in weather conditions.

Nomenclature:

I_{PH}	Photo current (A)
I_D	Diode current (A)
I_{SH}	Shunt current (A)
V_D	Diode voltage (V)
I_s	Reverse bias saturation current (A)
V_T	Thermal voltage (V)
T, T_{ref}	Cell and reference temperature (K)
k	Boltzmann constant (J/K)
K_i	Temperature coefficient (A/K)
R_c	Load resistance (Ω)
V_{oc}	Open circuit voltage (V)
V_{pv}	Output voltage of the PV module (V)
V_{DC}	Boost converter DC voltage (V)
γ	Ideality factor
ω	The pulse (rad/sec)
λ, λ_{ref}	Irradiance and reference irradiance (W/m^2)

References

- [1] F. Mohammadi, G.-A. Nazri, and M. Saif, "A bidirectional power charging control strategy for plug-in hybrid electric vehicles," *Sustainability*, vol. 11, no. 16, p. 4317, 2019. <https://doi.org/10.3390/su11164317>
- [2] R. Sims, "Energy for tomorrow's world. A renewable energy perspective," *Renewable Energy World*, vol. 3, no. 4, pp. 24-30, 2000.
- [3] C. Mehdipour and F. Mohammadi, "Design and analysis of a stand-alone photovoltaic system for footbridge lighting," *Journal of Solar Energy Research*, vol. 4, no. 2, pp. 85-91, 2019.

- [4] Y. Chaibi, M. Salhi, and A. El-Jouni, "Sliding mode controllers for standalone PV systems: Modeling and approach of control," *International Journal of Photoenergy*, pp. 1-12, 2019. <https://doi.org/10.1155/2019/5092078>
- [5] R. Alba-Flores, D. Lucien, T. Kirkland, L. Snowden, and D. Herrin, "Design and performance analysis of three photovoltaic systems to improve solar energy collection," in *In Proceedings of the IEEE SoutheastCon, St. Petersburg, FL, USA*, 2018, pp. 1–4.
- [6] M. Metry, M. B. Shadmand, R. S. Balog, and H. Abu-Rub, "MPPT of photovoltaic systems using sensorless current-based model predictive control," presented at the IEEE Transactions on Industry Applications, 2017.
- [7] D. Sera, L. Mathe, T. Kerekes, S. V. Spataru, and R. Teodorescu, "On the perturb-and-observe and incremental conductance MPPT methods for PV systems," *IEEE Journal of Photovoltaics*, vol. 3, no. 3, pp. 1070-1078, 2013.
- [8] N. Femia, G. Petrone, G. Spagnuolo, and M. Vitelli, "Optimization of perturb and observe maximum power point tracking method," *IEEE Transactions on Power Electronics*, vol. 20, no. 4, pp. 963-973, 2005.
- [9] L. Piegari and R. Rizzo, "Adaptive perturb and observe algorithm for photovoltaic maximum power point tracking," *IET Renewable Power Generation*, vol. 4, no. 4, pp. 317-328, 2010. <https://doi.org/10.1049/iet-rpg.2009.0006>
- [10] E. Bianconi *et al.*, "A fast current-based MPPT technique based on sliding mode control," in *In Proceedings of the 2011 IEEE International Symposium on Industrial Electronics, Gdansk, Poland, 27–30 June*, 2011, pp. 59–64.
- [11] K. Ali *et al.*, "Robust integral backstepping based nonlinear mppt control for a pv system," *Energies*, vol. 12, no. 16, pp. 1-20, 2019. <https://doi.org/10.3390/en12163180>
- [12] Y. Levron and D. Shmilovitz, "Maximum power point tracking employing sliding mode control," *IEEE Transactions on Circuits and Systems I: Regular Papers*, vol. 60, no. 3, pp. 724-732, 2013. <https://doi.org/10.1109/tcsi.2012.2215760>
- [13] J. Liu, *Sliding mode control using MATLAB*. Beijing, China: Academic Press, 2017.
- [14] J.-F. Tsai and Y.-P. Chen, "Sliding mode control and stability analysis of buck DC-DC converter," *International Journal of Electronics*, vol. 94, no. 3, pp. 209-222, 2007. <https://doi.org/10.1080/00207210601176692>
- [15] J. Liu, *Design, intelligent control design, and MATLAB simulation*. Singapore; Beijing, China: Springer, 2018.
- [16] D. G. Montoya, C. A. R. Paja, and R. Giral, "A new solution of maximum power point tracking based on sliding mode control," presented at the In Proceedings of the IECON 2013—39th Annual Conference of the IEEE Industrial Electronics Society, Vienna, Austria, 10–13 November, 2013.
- [17] S.-C. Tan, Y.-M. Lai, and K. T. Chi, "General design issues of sliding-mode controllers in DC–DC converters," *IEEE Transactions on Industrial Electronics*, vol. 55, no. 3, pp. 1160-1174, 2008. <https://doi.org/10.1109/tie.2007.909058>
- [18] F. Attivissimo, A. Di Nisio, M. Savino, and M. Spadavecchia, "Uncertainty analysis in photovoltaic cell parameter estimation," *IEEE Transactions on Instrumentation and Measurement*, vol. 61, no. 5, pp. 1334-1342, 2012. <https://doi.org/10.1109/tim.2012.2183429>
- [19] S. Cuk and R. Middlebrook, "Advances in switched-mode power conversion part II," *IEEE Transactions on Industrial Electronics*, vol. 30, no. 1, pp. 19-29, 1983. <https://doi.org/10.1109/tie.1983.356698>